Reconfigurable Blocker-Tolerant RF Front-end Filter with Tunable Notch for Active Cancellation of Transmitter Leakage in FDD Receivers

M. Naimul Hasan, Qun Jane Gu and Xiaoguang Liu
School of Electrical and Computer Engineering, University of California Davis, California, USA
Email: mhasan@ucdavis.edu

***Abstract*— A tunable N-path filter with an adaptive integrated notch is demonstrated for active cancellation of transmitter self-interference in frequency division duplexing (FDD) cellular systems. The proposed filter is a combination of N-path bandpass filter and a N-path bandstop filter, with the center frequency of the bandstop filter is tuned to the transmitting frequency to suppress transmit leakage. The passband of the filter is tunable from 0.4 GHz to 1.4 GHz. The gain of the filter is 17 dB. The rejection of the filter is 74.5 dB, where the notch is created. The NF of the filter is from 3.8–4.7 dB over the whole tuning range. The total power consumption of the filter is 36.4–56 mW. The channel bandwidth is 6.4 MHz and the out-of-band IIP3 is 21.2 dBm.**

I. Introduction

The growing demand of highly integrated multiband receivers for fourth-generation (4G)/fifth-generation (5G) wireless systems has driven the development of widely tunable filters for software defined radios. To reduce the cost and size of the transceiver chips, multiple dedicated narrowband radios must be replaced with one widely tunable radio. Off-chip, high-Q surface acoustic wave (SAW) filters are dedicated to suppress any out-of-band blockers in a conventional narrowband transceiver design. On the other hand, a wideband design has no selectivity and must withstand strong blockers as well as the wanted signal. In a frequency division duplexing system, the transmit (TX) signal is the most dominant blocker for the receiver. Several architectures have been proposed to handle large out-of-band (OOB) blockers and typically focus on 0-dBm continuous wave (CW) blockers. An out-of-band blocker is introduced at a frequency offset of 100 MHz in a long-term evaluation receiver, through TX leakage and TX self-interference as shown in Fig. 1 [1]. The frequency duplexer provides an isolation of 50 dB, which reduces the 30 dBm TX signal to -20 dBm in the primary receiver. Recent publications have shown tunable duplexers with high isolation between the transmit and receive signal paths [2]. On the other hand, the mobile device allows only 15 dB isolation between multiple antennas in a wireless system [1]. As a result, the received signal power is 12 dBm to secondary receivers, which significantly increases the IIP3 requirements. In a conventional architecture, a fixed SAW filter is inserted to suppress the TX leakage by 40 dB, and therefore, the OOB blocker power is reduced to -28 dBm as shown in Fig. 1(a) and the IIP3 requirement is relaxed. However, a fixed frequency SAW filter cannot be utilized in a wideband receiver.

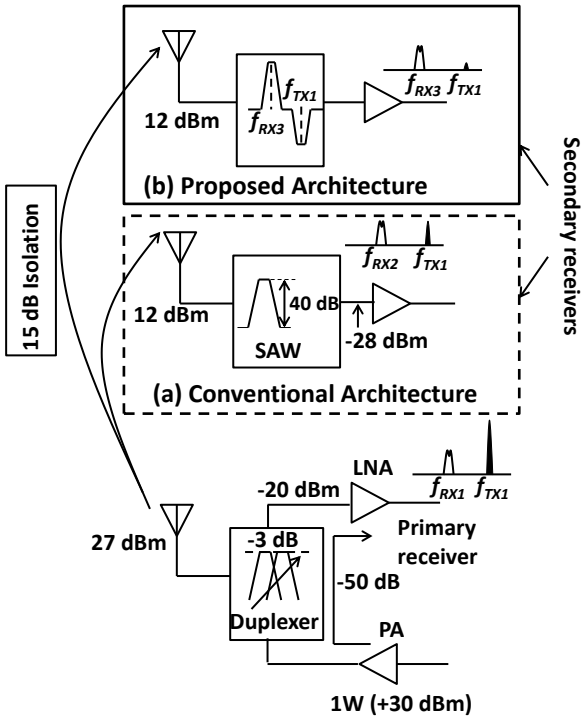

Fig. 1. Proposed TX leakage suppression (a) conventional architecture with SAW filter (b) proposed architecture with integrated notch.

Several architectures have been proposed to handle TX leakage in multiband radios. A combination of bandpass and band-reject filtering is independently proposed in [1], [3] to suppress TX leakage. The filter in [1] can only suppress the TX leakage when the frequency difference between TX and RX is at least 100 MHz, due to the wide bandwidth of the filter and the power consumption of the filter is high. A blocker resilient wideband receiver is proposed in [4], with two point cancellation of TX leakage and TX noise in receive band. However, this technique rely on precise amplitude and phase matching, which is sensitive to process, voltage and temperature variations. On chip bandpass filters with integrated tunable notch are presented in [1], [5]. However, the power consumption of the filters is high. A wideband LNA is proposed in [6] for digital TV applications. Due to the use

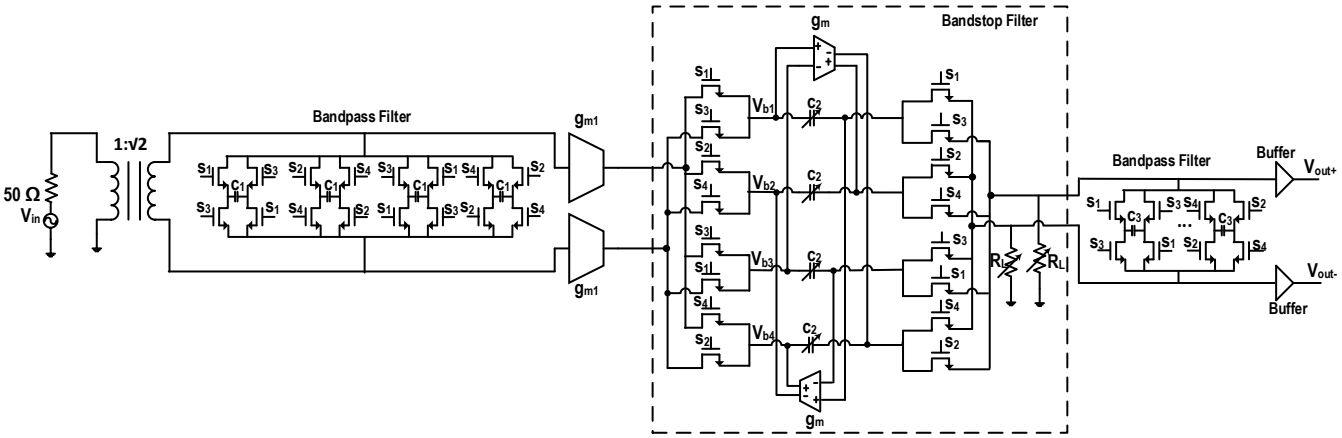

Fig. 2. Proposed Bandpass filter schematic with integrated tunable notch.

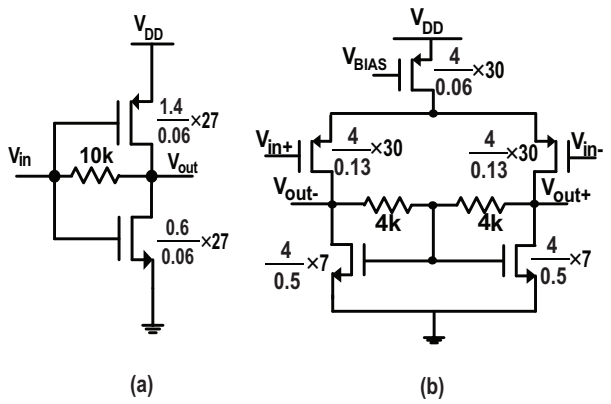

Fig. 3. (a) A self-biased inverter used as g_{m1} (b) g_{m} cells used in bandstop filter.

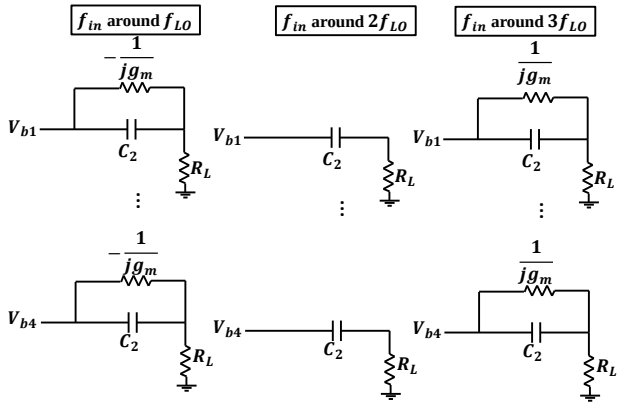

Fig. 4. Effective baseband admittance $Y_{BB}(s,k)(1 \leq k \leq 3)$ for the bandstop filter shown in Fig. 2.

of low supply voltage in modern CMOS process, a 0 dBm blocker will cause the LNA to clip, which increases noise and distortion in the receiver.

A low power tunable bandpass filter with an integrated adaptive notch is presented in this paper. The filter will be used in front of the LNA to handle large out-of-band blockers as shown in Fig. 1(b). In section II, the design of the proposed bandpass filter is demonstrated. Section III describes the simulation results and section IV concludes the paper.

II. Proposed Bandpass Filter Architecture

The proposed filter consists of two bandpass sections and one bandstop section between them. The bandpass sections are implemented with R-C configuration of N-path filters and the bandstop section is implemented with C-R configuration of N-path filters. The schematic of the proposed filter is shown in Fig. 2. A transconductor cell (g_{m1}) is used after the first bandpass section to increase the gain of the filter as well as to reduce the noise from subsequent stages. The center frequency of the bandstop filter is shifted by using feedforward and feedback gm cells. The gain of the bandstop section can be changed by varying the load resistance R_L. The transistor sizes used in the bandpass and bandstop sections are (W/L = 50 μm/60 nm) and (W/L = 40 μm/60 nm) respectively. The baseband capacitors used in the bandpass and bandstop sections are 50 pF and 8 pF, respectively. Two self-biased inverters are used as g_{m1} to increase the gain of the filter, as shown in Fig. 3(a). A fully differential architecture with resistive common mode feedback is used as the transconductor cell (g_m) in the bandstop filter as shown in Fig. 3(b) . The nominal value of load resistance, $R_L = 10\ k\Omega$.

A. Bandstop Filter Frequency Shifting

The primary idea of shifting the center frequency of a bandstop filter with respect to the switching frequency f_{LO} is described here. $g_m - C$ technique is used to shift the center frequency of the bandstop filter as shown in Fig. 2. Feedforward and feedback g_m cells are used at the baseband nodes ($V_{bi}, 1 \leq i \leq 4$) with differential capacitor baseband impedances to shift the center frequency of the bandstop filter. As a result, a bandstop filter can be cascaded with a bandpass filter to create an overall bandpass filter with an integrated notch.

The phase relation between the baseband node voltages, V_{bi} of a N-path filter can be described by $V_{bx} = V_{by}e^{\frac{jk\pi}{2}\times(x-y)}, [1 \leq (x,y) \leq N]$, where N is the number of clock phases. The equation only holds when f_{in} is around kf_{LO}. It is possible to find an effective baseband ad-

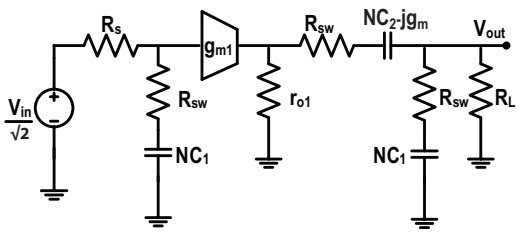

Fig. 5. A simplified half circuit schematic of the filter to calculate the overall transfer function of the filter (N=4).

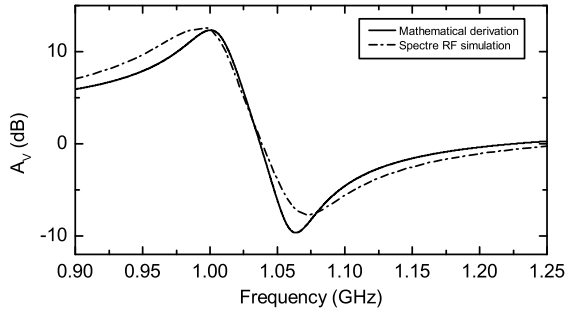

Fig. 6. Comparing SpectreRF simulation of the bandstop filter shown in Fig. 2 with mathematical derivation (5). ($R_{sw} = 20\Omega, g_m = 6.1\ mS, R_L = 10\ k\Omega$ and $C_2 = 8$ pF.)

mittance $Y_{BB}(s,k)$ due to the g_m cells between the baseband node voltages. $Y_{BB}(s,k)$ for f_{in} around $kf_{LO}[(1 \leq k \leq N-1)]$ for the bandstop filter shown in Fig. 2 is illustrated in Fig. 4. From Fig. 4, $Y_{BB}(s,1) = C_2(s - j\omega_{BB}), Y_{BB2} = sC_2$ and $Y_{BB}(s,3) = C_2(s + j\omega_{BB})$, where $\omega_{BB} = g_m/2C_2$. As a result, the center frequency of the baseband admittance is modified from 0 to ω_{BB} for $Y_{BB}(s,1)$ and $-\omega_{BB}$ for $Y_{BB}(s,3)$. Due to the exploitation of differential $g_m s$ with good common mode rejection, the center frequency of the baseband admittance does not change for $Y_{BB}(s,2)$. In N-path filters, the effective baseband admittance characteristics will be translated to $kf_{LO}, k \in Z$. Therefore, the center frequency of the filter shifts upward around f_{LO} and downward around $3f_{LO}$ by $g_m/4\pi C_2$. The filter operates similar to a conventional 4-path filter for input frequencies around $2f_{LO}$.

The bandstop filter transfer function is given by

$$H(s) = \frac{V_{out}(s)}{V_{in}(s)} = 1 - \sum_{k=-\infty}^{\infty} sinc^2\left(\frac{k\pi}{N}\right) \times G(s - jk\omega_{LO}, k) \tag{1}$$

where $G(s,k)$ is a HPF due to the combination of a baseband admittance $Y_{BB}(s,k)$ and a load resistance and described in

$$G(s,k) = \frac{NR_L}{NR_T Y_{BB}(s,k) + 1} \tag{2}$$

where N=4 in our case and $R_T = R_L + R_{sw}$
The transfer function of the filter around f_{LO} can be found by using two terms $(k = -1, 1)$ in (3)

$$H(s) = 1 - \frac{8}{\pi^2} \times (G(s - j\omega_{LO}, 1) + G(s - j\omega_{LO}, -1)) \tag{3}$$

where

$$\begin{aligned} G(s, \pm 1) &= \frac{NR_L Y_{BB}(s, \pm 1)}{1 + NR_T Y_{BB}(s, \pm 1)} \\ &= \frac{4R_L(sC_2 \pm jg_m)}{1 + 4R_T(sC_2 \pm jg_m)} \end{aligned} \tag{4}$$

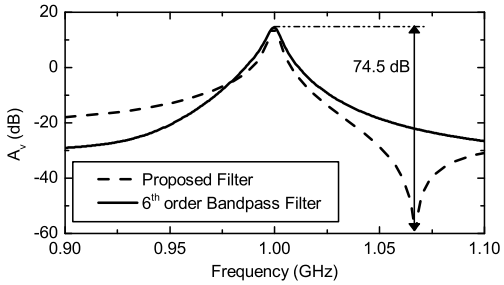

Fig. 7. Comparison between all pole filter and the proposed filter.

Therefore, $H(s)$ will be

$$\begin{aligned} H(s) &= 1 - \frac{8}{\pi^2} \times \left(\frac{4R_L C_2(s - j\omega_{LO}) - j4g_m R_L}{1 + 4R_T C_2(s - j\omega_{LO}) - j4g_m R_T}\right) \\ &\quad - \frac{8}{\pi^2} \times \left(\frac{4R_L C_2(s + j\omega_{LO}) + j4g_m R_L}{1 + 4R_T C_2(s + j\omega_{LO}) + j4g_m R_T}\right) \\ &= 1 - \frac{16R_L}{\pi^2 R_T} \times \frac{s^2 + \left(\frac{g_m}{2C_2} + \omega_{LO}\right)^2}{s^2 + \frac{2s}{R_T C_2} + \omega_{LO}^2} \end{aligned} \tag{5}$$

The center frequency of the bandstop filter is shifted to $\frac{g_m}{4\pi C_2}$. Depending on whether g_m is positive or negative, the frequency shifting is negative or positive, respectively. As a result, the notch frequency can be shifted to either side of the filter center frequency.

B. Transfer Function of the Filter

The overall transfer function of the filter can be calculated from Fig. 5. Assuming, $R_L \gg R_{sw}$, we can use (5), to find the transfer function of the bandstop filter by replacing R_L with $\frac{R_{sw} + j\omega NC_1}{j\omega NC_1}$. The overall transfer function is described in (6), where

$$H_1(s) = g_{m1} r_{o1} \times \frac{R_{sw}(1 + sNC_1)}{R_{sw} + sNC_1(R_s + R_{sw})} \tag{7}$$

The transfer function of the filter is compared with the SpectreRF simulation in Fig. 6 for $R_{sw} = 20\ \Omega$, $R_L = 10\ k\Omega$, $C_2 = 8$ pF, and $g_m = 6.1$ mS. The notch frequency is shifted in the SpectreRF simulation due to the bottom plate parasitic capacitance of the baseband capacitance.

III. Simulation Results

The proposed filter is designed using 65 nm CMOS technology. The baseband capacitors are realized with MIM capacitors and the resistors are realized with N+ poly resistor

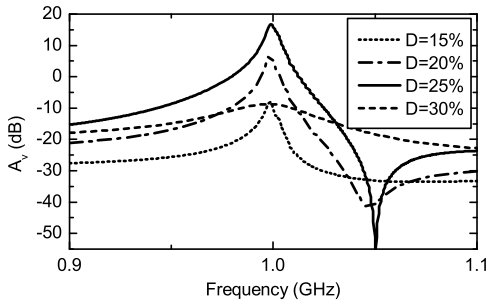

Fig. 8. The transfer function of the filter with duty cycle variations.

$$H_{tot}(s) = H_1(s)\left(1 - \frac{16}{\pi^2} \times \frac{1 + sNC_2R_{sw}}{1 + sNR_{sw}(C_2 + C_1)} \times \frac{s^2 + \left(\frac{g_m}{2C_2} + \omega_{LO}\right)^2}{s^2 + \frac{2s}{R_TC_2} + \omega_{LO}^2}\right) \quad (6)$$

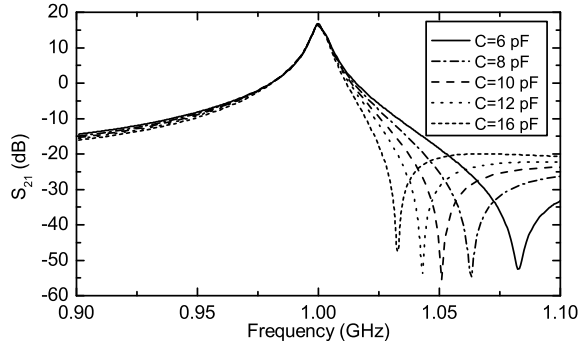

Fig. 9. The notch frequency is shifted by changing the bandstop filter capacitors

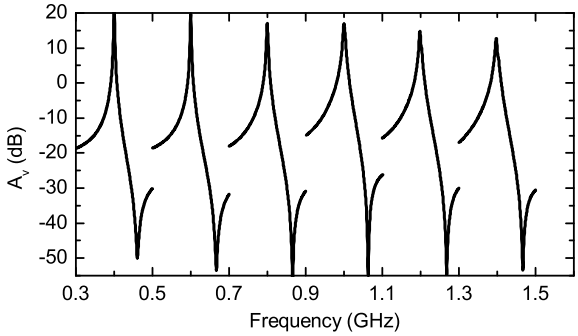

Fig. 10. The simulated transfer function of the filter shown at every 200 MHz over the frequency range from 0.4 GHz to 1.4 GHz.

without salicide. The proposed filter is compared with an all pole 6^{th} order conventional Butterworth filter as shown in Fig. 7, considering that the two filters occupy similar areas. The proposed filter has 40 dB more rejection at 60 MHz offset compared with the all pole filter. Due to the high attenuation at a particular frequency and the tunability, the proposed filter can significantly block the strong transmitter in the receive band. The filter has 17 dB gain provided by the $g_{\rm m}$ cells as shown in Fig. 7 with passband ripple of 0.4 dB. The transfer function of the filter with different clock duty cycle (D) is shown in Fig. 8. Reducing the duty cycle from 1/N results in higher input impedance for frequencies far away from the switching frequency, which translates to less rejection. On the other hand, if D $>$ 1/N, two switches will be on at the same time, which results in undesired charge sharing between capacitors. The figure clearly shows that the maximum notch depth is achieved for duty cycle=25%. The notch frequency can be shifted by changing the bandstop filter capacitance (C_2). The transfer function of the filter with different notch capacitance is shown in Fig. 9, as the notch capacitance is changed from 6 pF to 16 pF. Due to the tunability of notch frequency, the proposed filter can handle strong out of band blockers as well as the TX frequency. The filter is tunable from 0.4 GHz to 1.4 GHz and the transfer function over the whole tuning range is shown in Fig. 10. The gain of the filter drops at higher frequency. The 3-dB BW of the filter is 6.4 MHz. The power consumption from the analog blocks is 34.4 mW and the digital power varies from 1.8 to 21.6 mW. The in-band IIP3 of the filter is -7.8 dBm. The simulated out-of-band IIP3 (OOB) of +21.2 dBm is obtained at $\triangle f$ of 60 MHz and $f_{\rm lo}$ of 1 GHz. The filter is compared with state-of-the-art integrated filters in Table I.

TABLE I

COMPARISON TABLE

	Luo [1]	Zhou [4]	Chen [5]	This work
Circuit Type	Filter	Receiver	Receiver	Filter
CMOS Tech.	45 nm [SOI]	65 nm	65 nm [LP]	65 nm
Frequency range [GHz]	0.2–3.6	0.3–1.7	0.1–1	0.4–1.4
Gain [dB]	-4	19–34	23	17
Attenuation @ offset	41 [100 MHz]	30 [20 MHz]	33 [50 MHz]	74.5 [60 MHz]
BW [MHz]	$>$ 80	2–76	12	6.4
NF [dB]	2.8–4.5	4.2–5.6	5.5–7.6	3.8–4.7
NF with 0-dBm blocker @ offset	4.1 dB @ 100 MHz	-	-	5.84 dB @ 60 MHz
Blocker P1dB	$>$ 10 dBm	$>$ +2 dBm	-6 dBm	+4 dBm
IIP3 (OOB)	29 dBm	12–14 dBm	5.5–8.7 dBm	21.2 dBm
$V_{\rm DD}$ [volts]	1.5	1.2	1.2	1.2
Power [mW]	183–303	146.6–155	74–146	36.4–56

IV. Conclusion

A low power tunable bandpass filter with integrated tunable notch is presented. The proposed filter can be integrated into the RF transceiver chips. The filter can handle large out-of-band blockers at a particular offset by creating a notch at that frequency. Due to the tunability of the bandstop filter and also the notch depth, the receiver is not desensitized by strong blockers including the transmitter. The notch frequency can be tuned to both sides of the filter center frequency.

References

[1] C. Luo, P. Gudem, and J. Buckwalter, "A 0.2–3.6-GHz 10-dBm B1dB 29-dBm IIP3 Tunable filter for transmit leakage suppression in SAW-less 3G/4G FDD receivers," *IEEE Transactions on Microwave Theory and Techniques*, pp. 1–11, 2015.

[2] S. Abdelhalem, P. Gudem, and L. Larson, "Hybrid transformer-based tunable integrated duplexer with antenna impedance tracking loop," in *Custom Integrated Circuits Conference (CICC), 2013 IEEE*, 2013, pp. 1–4.

[3] M. Hasan, S. Aggarwal, Q. Gu, and X. Liu, "Tunable N-path RF front-end filter with an adaptive integrated notch for FDD/co-existence," in *2015 IEEE 58th International Midwest Symposium on Circuits and Systems (MWSCAS)*,, 2015, pp. 1–4.

[4] J. Zhou, A. Chakrabarti, P. Kinget, and H. Krishnaswamy, "Low-noise active cancellation of transmitter leakage and transmitter noise in broadband wireless receivers for FDD/Co-existence," *IEEE Journal of Solid-State Circuits*, vol. 49, no. 12, pp. 3046–3062, 2014.

[5] R. Chen and H. Hashemi, "Dual-carrier aggregation receiver with reconfigurable front-end RF signal conditioning," *IEEE Journal of Solid-State Circuits*, vol. 50, no. 8, pp. 1874–1888, 2015.

[6] J.-Y. Bae, S. Kim, H.-S. Cho, I.-Y. Lee, D. Ha, and S.-G. Lee, "A CMOS wideband highly linear low-noise amplifier for digital TV applications," *IEEE Transactions on Microwave Theory and Techniques*, vol. 61, no. 10, pp. 3700–3711, 2013.